A STUDY OF FUEL SYSTEM INTEGRITY AND ELECTRIC SAFETY OF HFCV

Kwang-Bum LEE
Jae-Wan LEE
Jong-Soo KIM
Gee-Joong YONG
Korea Automobile Testing and Research Institute
Republic of Korea
Paper Number 11-0412

ABSTRACT

This research consists of two parts. The first part is to evaluate the fire risk due to the hydrogen leakage or diffusion from the hydrogen storage system. The second part is to verify compliance with the fuel leakage limit of a hydrogen fuel cell vehicle in the event of collision. To evaluate the fire risk of the fuel storage and delivery system in a hydrogen fuel-cell vehicle, sensors were installed at locations where leaking hydrogen was likely to be trapped. These sensors were installed in the engine compartment, the occupant compartment and in the rear of a vehicle. The fuel processing system and fuel-cell stacks were located in the engine compartment. The behavior of leaking hydrogen was investigated when a vehicle was at rest, moving, and after shut-down caused by hydrogen leakage. In some area the concentration reached up to 4%. The optimization of number of sensors and locations was also investigated for effective detection.

To assess the vehicle fuel system integrity and electrical safety in the event of a crash, three different crashes were carried out. One full frontal impact test at the speed of 48 km/h, one side impact test at the speed of 50 km/h with a deformable moving barrier and one rear impact test at the speed of 48 km/h with a moving barrier were conducted. The hydrogen fuel storage systems were filled to 90 % of the nominal working pressure with helium gas at each test. Even though the hydrogen fuel cell vehicle subject to tests was equipped with crash sensors that enabled the high pressure valve of the storage container to be closed automatically in the event of a crash, all crash sensors were removed to simulate severe test conditions in these experiments. After each crash, the amounts of hydrogen leakages were measured, and electrical safety were examined.

In this experiment 8 research institutes, including the Korea Automobile Testing and Research Institute, Hyundai Motor Company, took part. This project was supported by the Ministry of Land, Transportation and Maritime Affairs of the Republic of Korea.

INTRODUCTION

The purpose of this research is to secure the safety of the fuel storage and delivery system in a hydrogen fuel cell vehicle by assessing the danger with sensors installed where leaking hydrogen is likely to be trapped. In the hydrogen fuel-cell vehicle, the storage container is located in the rear of a vehicle and the fuel processing system (FPS) and fuel-cell stacks are located in the engine compartment. The hydrogen fuel from the storage containers is supplied to the fuel cell stacks, where electricity is generated, through FPS with a series of pressure regulators that reduce the pressure to approximately 1 MPa before entering the fuel cell stack. Excessive hydrogen is returned to the FPS through the gas recovery system or discharged. Hydrogen is likely to leak from the high pressure components (35 MPa) and low pressure components (1 MPa) of the storage system, fuel cell stacks, and piping of the hydrogen fuel delivery system.

In this study, the behavior of leaking hydrogen was investigated when a vehicle was at rest, when a vehicle was moving, and after a vehicle was shut-down because of the hydrogen leakage. A hydrogen fuel cell vehicle uses hydrogen with high pressure (35 or 70 MPa) and a battery above 400 Volts. Due to this nature the safety of a hydrogen fuel cell vehicle, against the risk of fire, electric isolation failure or electric shock, should be secured in the event of a collision. There is no provision regarding the hydrogen leakage of a hydrogen fuel cell vehicle in Article 91 (Fuel System) in the Korean Motor Vehicles Safety Standards. In this study the Japanese Motor Vehicles Safety Standards (Attachment 17) and GTR Draft ware utilized to evaluate the fuel system integrity of a sport utility vehicle by measuring the

pressure drop when the vehicle was impacted.

RESEARCH

Research for the behavior of leaking hydrogen

Leakage test for a vehicle at rest

(A) Locations of leaking points

Eleven leaking points were chosen, mainly fittings near the storage system. Eight leaking points were fittings connected directly to the storage system and three leaking points connected directly to the FPS. The hydrogen flow rate was 40 liters/min (LPM) which was the maximum allowable limit before the excess flow valve (EFV) began to operate. The experiments were continued until the hydrogen sensors detected 4 % hydrogen in air under the condition that the maximum post crash hydrogen leakage was equivalent to maximum post crash leakages of 120~130 LPM from gasoline vehicles.

Twelve on-board hydrogen sensors were located on the floor near the storage container. Outside the vehicle eight hydrogen sensors were installed at 1.5 m high around the vehicle where a human might smell the hydrogen and nine hydrogen sensors were installed at 3 m high around the vehicle, taking into consideration of parking area. Considering the possibility of hydrogen leakage into the passenger compartment, one near the stack, one near the FPS, one on the instrument panel and two in the interior were installed. With thirty four sensors in total the concentration of leaking hydrogen and response time were measured.

(B) Test Results of Hydrogen Leakage

Test results were collected from two areas, the underbody and engine compartment of a hydrogen fuel cell vehicle. Hydrogen leakage was simulated along the direction of hydrogen leakage at each fitting on the underbody. Figure 1 shows that hydrogen concentrations at Sensors No. 20, 31 and 32, which were measured with respect to the directions and flow rates at 8 leaking points on the underbody. It was expected that above 3 sensors were likely to detect any leakage from the underbody. Especially Sensors No. 31 and 32 were originally installed by the manufacturer and Sensor No. 32 covered any leakage from all area. Sensor No. 20 was found to detect any leakage faster and from the wider area than Sensor No. 31.

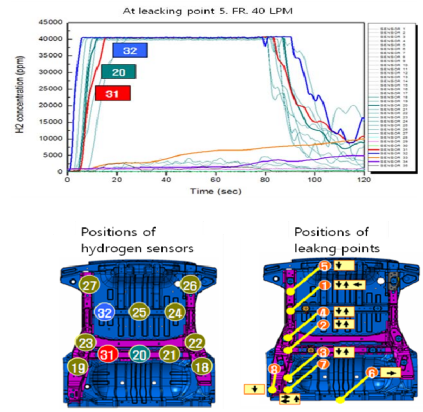

Figure 1. Hydrogen concentration at Sensors No. 20, 31 and 32, measured with respect to the directions and flow rates at 8 leaking points on the underbody.

Figure 2 shows the sensor locations and leaking points in the engine compartment. Hydrogen leaked from 3 points and measurements were made at the sensors shown in Figure 3. Sensors No. 28, 29, and 30 were installed near the stack, FPS and instrument panel respectively by the manufacturer.

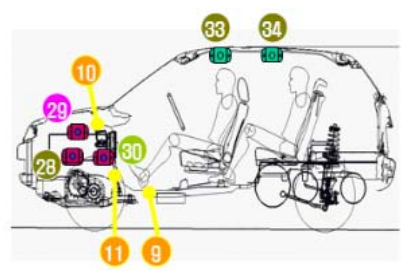

Figure 2. The sensor locations and leaking points in the engine compartment.

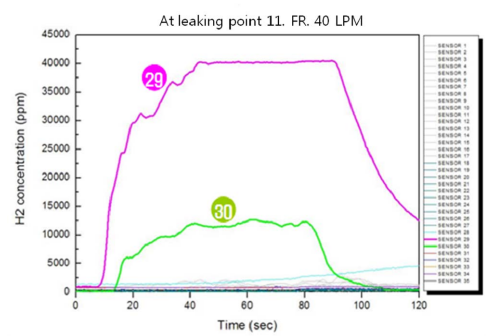

Figure 3. Hydrogen concentration at each sensor in the engine compartment. The flow rate was 40 LPM forward.

The results show that Sensor No. 29 in FPS was found to detect any leakage faster and more effectively

than Sensor No. 30 on the instrument panel in any case. It was concluded that Sensor No. 29 in FPS was located at the optimum location and Sensor No. 30 on the instrument panel might be redundant and removed.

Leakage test for a moving vehicle

(A) Simulation of leakage

Before the experiment, the behavior of hydrogen flow was analyzed by simulation for a moving vehicle. Hydrogen was supposed to leak from high pressure lines at the maximum allowable limit of 131 LPM [3)] while a vehicle was moving at 36 km/h. The simulation package was STAR-CCM+. Figure 4 shows the simulation results.

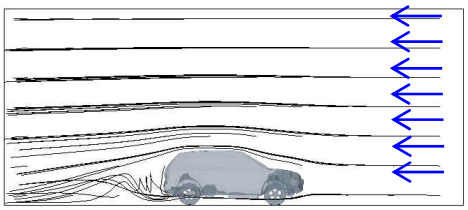

Figure 4. Simulation of hydrogen leakage for a moving vehicle.

Figure 5 shows that hydrogen concentration in air of 4 % or more was localized near leaking points. Because hydrogen was rapidly diffused to the outside by outside air flow, other sensors barely detected hydrogen.

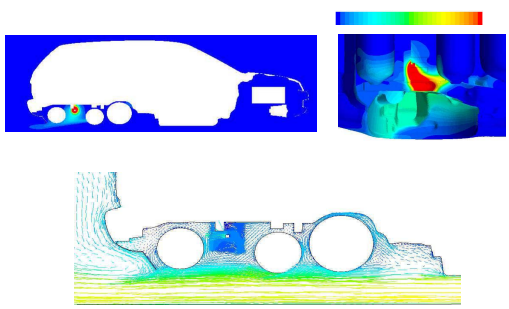

Figure 5. Analysis of hydrogen leakage for a moving vehicle.

(B) Leakage Experiment for a moving vehicle

In this experiment SUV hydrogen fuel cell vehicle was used. The head wind of 10 m/sec was blowing to the vehicle with a fan to simulate driving. Eleven possible leaking points at the storage system and delivery subsystem were shown in Figure 6. Leaking points were mainly connections. At these leaking points hydrogen was leaking with the hydrogen leakage simulation system.

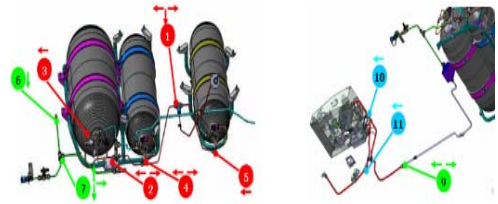

Figure 6. Possible leaking points.

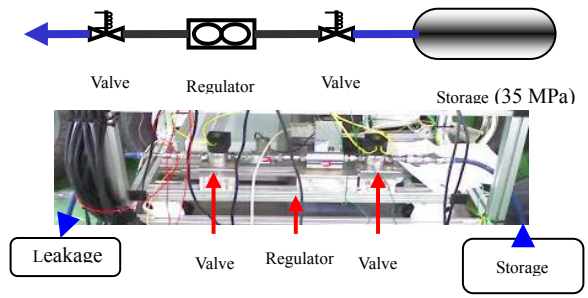

Figure 7. Hydrogen leakage simulation system.

To detect leaking hydrogen 34 sensors in and out of the vehicle were installed as in Figure 8. At each leaking point hydrogen leakage was controlled at 10, 40, and 131 LPM. The flow rates were set at 10 LPM for a low flow rate, at 40 LPM for the onset of Excess Flow Valve (EFV), and 131 LPM for the maximum hydrogen leakage based on the heat energy equivalent to maximum post crash leakages from gasoline vehicles specified in US FMVSS 301. The direction of leakage from each leaking point was set for the front (FF), rear (RR) and side (LH, RH).

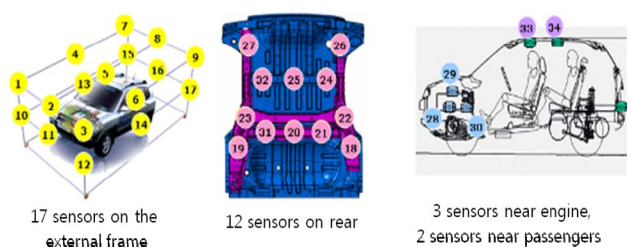

Figure 8. Locations of 34 sensors.

The test consisted of two parts. The first part was from the beginning of leakage to the point where a hydrogen concentration in air by volume reached 2 % (the onset of EFV, where the car was shut-down). Time to reach 2 % concentration was measured for this part. The second part was after the shut down. At 10 seconds and 60 seconds after the shut-down, a hydrogen concentration in air was measured. The duration period was measured, which meant the time for the hydrogen

concentration in air to stay higher than 4 % after shut-down.

In case of a stationary vehicle a large amount of hydrogen was expected to leak if EFV shut-down the valve on detecting a hydrogen concentration in air of 2 %. The delay time between shut-down and detection of 2 % should be reconsidered. However, because the conditions for shut-down were related to emergency, the conditions should be reviewed from many aspects.

On detecting a hydrogen concentration in air of 2 % by volume on any leaking points, the vehicle was shut-down. Though a concentration might reach 4 % within 10 seconds after detecting, concentrations everywhere dropped below 4 % after one minute. The results from this study will be a ground to establish a guide for the desirable number and locations of sensors to be installed in and out of a vehicle.

Crashworthiness test and Analysis

Vehicle Preparations

The purpose of this test was to assess the fuel system integrity in the event of a rear collision. The mock-up vehicle was impacted the frontal and the rear impact test of 48 km/h, the side impact test of 50 km/. After the crash the amount of hydrogen leakage were examined. The mock-up vehicle was equipped with the hydrogen fuel storage system built by the manufacturer. Additional structural change was made to adjust weight distribution equivalent to the related parts such as the fuel cell stack, electric motors, batteries, etc. The hydrogen fuel storage system was filled to 90 % of nominal working pressure with helium gas. Air tightness was verified before the test. The hydrogen fuel cell vehicle is equipped with crash sensors that enabled the high pressure valve of the storage container to be closed automatically after a crash. However in this experiment all crash sensors were removed to simulate severe test conditions. [1),2),4),7),9)]

Verification of compliance and Analysis

(A) Overview: Article 91(Fuel System) in the Korean Motor Vehicle Safety Standards(KMVSS) applies to hybrid vehicles, electric vehicles and vehicles using gasoline, diesels and CNG. Passenger vehicles and buses with GVW of 4.5 tons or less are subject to this regulation. These vehicles shall meet fuel spillage requirements after and during the crash. In any rollover test, from the onset of rotational motion, vehicles shall meet fuel spillage requirements for the first 5 min of testing at each successive 90° increment on the longitudinal center line of a vehicle.

(B) Relevant standards: Japanese Safety Standard Attachment 17 (Technical Standard for Fuel Leakage in Collisions, etc.) and Attachment 100 (Technical Standard for Fuel Systems of Motor Vehicles Fueled by Compressed Hydrogen Gas). This standard applies to the fuel tank and fuel lines of vehicles using compressed hydrogen gas in the events of frontal and rear collisions. Hydrogen leakage shall not exceed 131 LPM (118 LPM at GTR Draft) for the first 60 min after the impact.

(C) Test procedures and Methods: Based on Article 91 (Fuel System) in the Korean Motor Vehicles Safety Standards and the Japanese Motor Vehicles Safety Standards (Attachment 17 & 100), amount of fuel leakage and body-acceleration were measured.

- Pressure sensors were installed in the test vehicle where hydrogen fuel system including the hydrogen tank was installed.
- The Fuel tank and fuel system was filled with helium gas at high (33 MPa) and low (1 MPa) pressure parts. Soap bubbles were used to test the leakage.
- The mass of test vehicle consisted of the unloaded vehicle and two dummies, equivalent to 156 kg.
- The Side impact of the moving barrier was 950kg.
- The Rear impact of the moving barrier was 1,805kg.
- Acceleration sensors were installed at the vehicle's center of mass, right and left of B-pillar and in the fuel tank.
- The hydrogen fuel storage system was filled to 90 % of nominal working pressure with helium gas.
- The degree of deformation was measured in vehicle's body and around fuel tank before and after the test.
- The temperature was measured around the test vehicle.
- High speed cameras were used when necessary.

Test results

(A) The Frontal Impact Test

- Pressure measurement after test

Figure 9 is the pressure measurement after the test. The high (31.5 MPa) and low (0.8 MPa) pressure stayed constant showing no reduction in pressure.

- Measurement of deformation in body and area near the fuel tank

The biggest deformation, 41.69 mm occurred along the longitudinal center line, which was measured the hydrogen receptacle points. In the area around the fuel tanks, brackets supporting the front fuel tank showed the biggest damage, 41.38 mm.

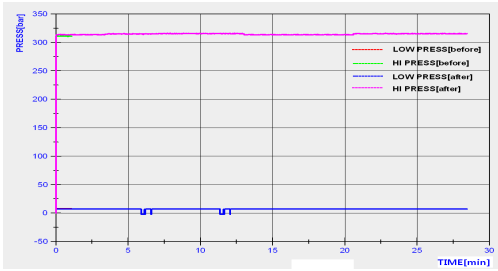

Figure 9. Pressure measurement after the frontal impact test.

- Pictures showing the test

Pictures in Fig. 10 show the vehicle of frontal impact test scene. After the test, the occupant safety requirements met KMVSS article 91, 102.

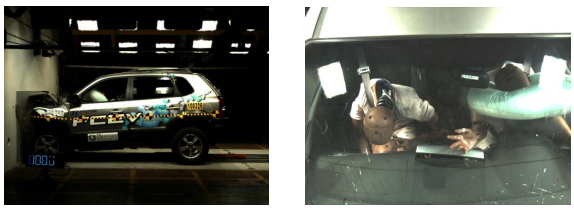

Figure 10. The test vehicle of frontal impact test.

- Test data
  - Acceleration of the vehicle

Figure 11 shows locations of acceleration sensors.

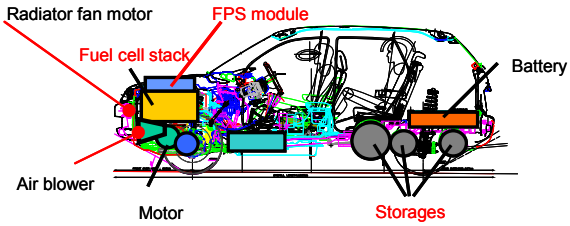

Figure 11. Locations of acceleration sensors.

Figure 12 shows the acceleration measured at body, B-pillar, storages of the vehicle. Figure 12 is a graph comparing the measured acceleration values for B-pillar on the left and the test car's center of gravity and the measured acceleration value for the storages. The value of any acceleration represents the vehicle traveling direction (X-axis) and the value of the acceleration waveform (pulse) and the maximum were similar to the body and storages. The middle of the storage was the highest value of acceleration.

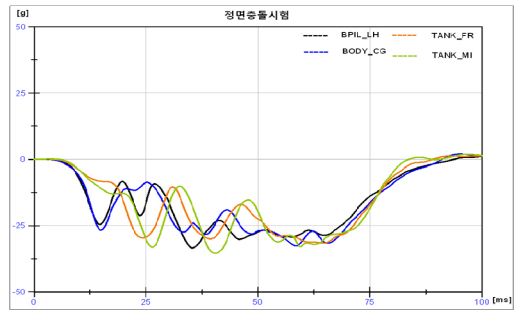

Figure 12. Acceleration graphs of the B-pillar and Body.

- Electrical safety measures of post crash

Picture in Figure 13 show the insulation resistance measurement scene. After the Frontal Impact Test, 3.1 kΩ/V values for the battery and body insulation resistance measurement were to meet the criteria. (100Ω/V) [1),3),5),6),8)]

Figure 13. Insulation resistance measurement.

(B) The Rear Impact Test

- Pressure measurement after test

Figure 14 is the pressure measurement after the rear impact test. The high (33 MPa) and low (1 MPa) pressure stayed constant showing no reduction in pressure.

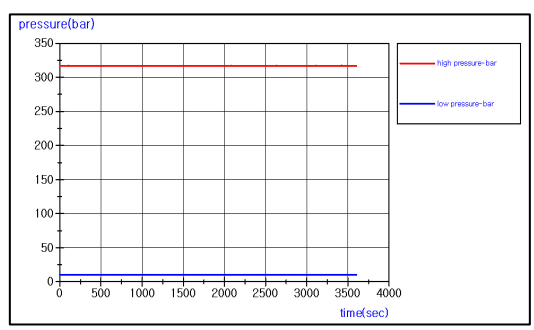

Figure 14. Pressure measurement after the rear impact test.

- Measurement of deformation in body and area near the fuel tank

Table 1 show the amount of deformation in the body and in the area near the fuel tank. The biggest deformation, 245 mm occurred along the longitudinal center line, which was measured between the mid points of front and rear bumpers. In the area around the fuel tanks, brackets supporting the rearmost fuel tank showed the biggest damage, 172 mm.

Table 1. Measurement of body deformation

Measured length	Deformation (mm)
Body length along longitudinal center line	245.1
Body length at one quarter line from the left	243.3
Body length at left end of bumper	200.3
Body length at one quarter line from the right	238.3
Body length at right end of bumper	236.9

- Pictures showing the test

Pictures in Figure 15 show the vehicle before and after the test. Other than some weights to adjust the total weight of the vehicle, no additional system was installed in the engine compartment and the luggage compartment of the vehicle. After the test, the rearmost fuel tank was displaced toward the front by 172 mm, but not damaged.

Figure 15. Rear-right view of the test vehicle before and after test.

- Test data
  - Acceleration of the vehicle

Figure 16 shows the acceleration measured at left/right sides of B-pillar of the vehicle. The maximum acceleration was 27.2 g at 23.8 msec on the left side of B-pillar, 21.9 g at 39.7 msec on the right side B-pillar.

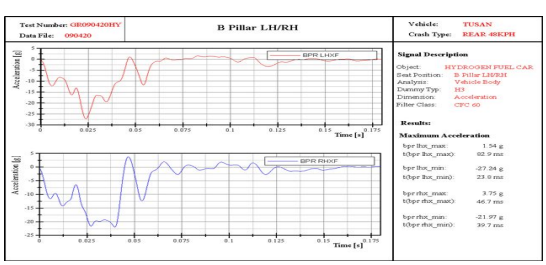

Figure 16. Acceleration graphs of the B-pillar.

- Acceleration of fuel tank

Figure 17 and Figure 18 show the acceleration for each fuel tank. The first tank from the front showed maximum acceleration 89.4 g at 26.8 msec. the sensor at the middle one was broken due to the damage of lower part of the vehicle resulting in no measurement. The rearmost tank showed 102.2 g at 14.8 msec.

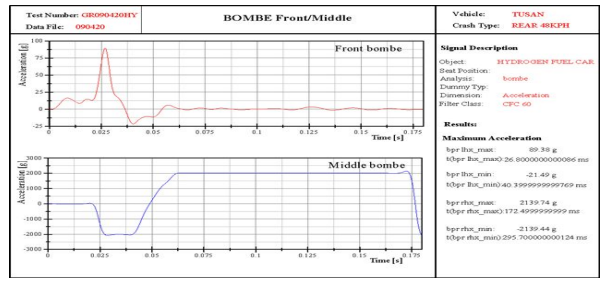

Figure 17. Acceleration graphs of the first and the second fuel tanks.

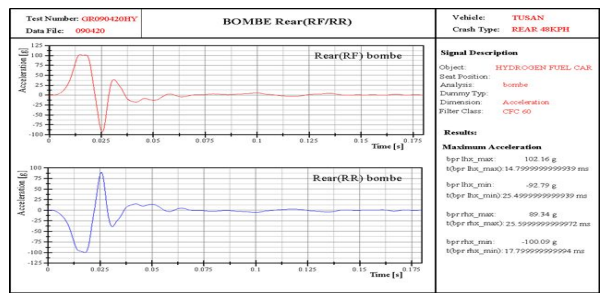

Figure 18. Acceleration graph of the rearmost fuel tank.

- Rupture test of hydrogen fuel tank [7),10)]

It was possible that the shock from the impact caused some deterioration to the tank's function to be filled at high pressure repeatedly. The tank was ruptured at the pressure of 103.8 MPa. This was high enough to satisfy the criteria, 82.2 MPa, which was 2.35 times the nominal working pressure, the EIHP standard. The tank withstood the pressure cycling test of over 11,250. Therefore there was no functional deterioration in the tested fuel tanks.

Figure 19. Rupture test of hydrogen fuel tank after rear test.

(C) The Side Impact Test

 Pressure measurement after test

Figure 20 is the pressure measurement after the test. The high (31.5 MPa) and low (0.8 MPa) pressure stayed constant showing no reduction in pressure.

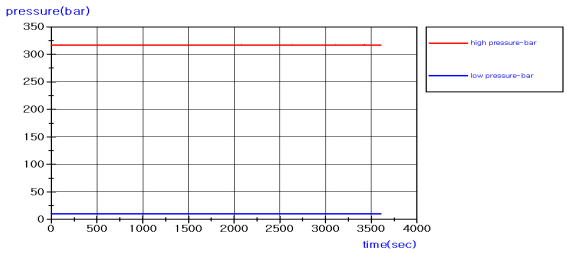

Figure 20. Pressure measurement after the side test.

 Measurement of deformation in body and area near the fuel tank

Around the fuel tank and body is measured the lateral deformation. The biggest deformation, 168 mm occurred displacement which was measured H-point height of the baseline on the left side door and the right side door. Deformation around the fuel tank caused the most part is the fuel inlet area. Deformation in the direction perpendicular to the vehicle central longitudinal section is 39mm.

 Pictures showing the side test

Pictures in Figure 21 show the vehicle of side impact test scene. After the test, the occupant safety requirements met KMVSS article 91, 102.

Figure 21. The test vehicle of side impact test.

 Test data

 Acceleration of the vehicle

Figure 22 shows the acceleration measured at body, motor, stack, battery, FPS of the vehicle. Accelerations at stack and FPS were relatively lower because they were located in front of vehicle. The motor was the highest value of acceleration.

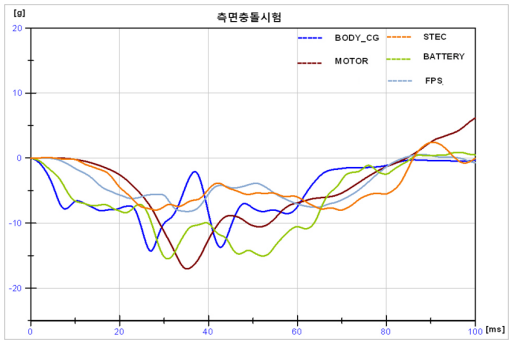

Figure 22. Acceleration graphs of the body and others.

ⓑ Electrical safety measures of post crash

Picture in Figure 23 show the insulation resistance measurement scene. After the Frontal Impact Test, 4.8 kΩ/V values for the battery and body insulation resistance measurement were to meet the criteria. (100Ω/V) [1),3),5),6),8)]

Figure 23. Insulation resistance measurement.

© Electrical safety measures of in use

· Protection against direct contact

- The live parts inside the passenger compartment or luggage compartment [5),6)]

Using the IPXX D test finger, evaluation tests were carried out passenger compartment and supercapacity of luggage compartment.

Figure 24. IPXX D (test wire) and luggage evaluation.

- The live parts in areas other than the passenger compartment or luggage compartment [5),6)]

Using the IPXX B test finger, evaluation tests were carried out junction box of bonnet.

Figure 25. IPXX B (test wire) and bonnet evaluation.

· Isolation Resistance

The minimum of electrical insulation resistance should be more than 100 Ω/V (DC), 500 Ω/V(AC). [5),6)] Insulation resistance of AC and DC input and output with both the vehicle chassis was evaluated above 1.28 kΩ /V

Figure 26. Insulation resistance evaluation.

· Protection against indirect contact

The test criteria of Protection against indirect contact should be less than 100 mΩ. [5),6)] The high voltage box enclosure and the Chassis was evaluated 5.4 mΩ. The supercapacitor enclosure and the chassis was evaluated 45.4 mΩ.

Figure 27. The high voltage box enclosure and the chassis evaluation.

Figure 28. The supercapacitor enclosure and the chassis evaluation.

CONCLUSIONS

The behavior of leaking hydrogen was investigated when a vehicle was at rest, when a vehicle was moving, and after the vehicle was shut-down because of the hydrogen leakage. To investigate the behavior of the leaking hydrogen, flow was analyzed by simulation for a moving vehicle. The simulation package was STAR-CCM+. In the simulation the vehicle was moving at 36 km/h and the hydrogen was supposed to leak from high pressure lines at the maximum allowable leakage of 131 LPM. During the test, the head wind of 10 m/sec was blowing to the vehicle with a fan to simulate driving. Thirty four sensors were installed at points where the leaking hydrogen was expected to be trapped. The test was done at leaking rates of 10, 40 and 131 LPM.

Next, in the frontal impact test, the test vehicle was impacted 48 km/h full frontal impact with hybrid Ⅲ 50 % male dummies. The test showed no leakage although some body deformation occurred. The electrical isolation and electrical continuity met the requirements in-use and post-crash. In case of frontal post-crash, it is not easy to measure electrical continuity because of severe damage to frontal part of vehicle.

In the rear impact test, the test vehicle was impacted form the rear by a moving barrier at the speed of 48 km/h. The test showed no leakage although some body deformation occurred. The results of tank rupture test also satisfied the safety standard of high pressure tank (EIHP). Functional deterioration of tank was not observed.

In the side impact test, the test vehicle was impacted 50 km/h side impact with deformable moving barrier (950 kg). The test showed no leakage although some body deformation occurred. The electrical isolation and electrical continuity met the requirements in-use and post-crash.

ACKNOWLEDGEMENT

This research was supported by a grant (07-Transport System-Furture-02) from Transportation System Innovation Program funded by the Ministry of Land, Transport and Maritime Affairs, Republic of Korea.

REFERENCES

[1] Korean Motor Vehicles Safety Standards, Article 91(Fuel Device) & 102(Passenger Protection at the Time of Collision)

[2] Japanese Motor Vehicles Safety Standards (Attachment 17) Fuel Leakage in Collision

[3] Japanese Motor Vehicles Safety Standards (Attachment 100 : Technical Standard for Fuel Systems of Motor Vehicles Fueled by Compressed Hydrogen Gas)

[4] http://www.unece.org/trans/main/wp29/grsp/informal group on hfcv-SGS

[5] http://www.unece.org/trans/main/wp29/grsp/informal group on electric safety

[6] UN ECE Regulation No. 100 "Uniform Provisions Concerning The Approval Of Battery Electric Vehicles With Regard To Specific Requirements for The Construction AND Functional Safety"

[7] UN ECE Regulation No. 110 "SPECIFIC COMPONENTS OF MOTOR VEHICLES USING COMPRESSED NATURAL GAS (CNG) IN THEIR PROPULSION SYSTEM"

[8] FMVSS 305, NHTSA. "Electric-powered vehicles: electrolyte spillage and electrical shock protection"

[9] FMVSS 303, NHTSA. "Fuel system integrity of compressed natural gas vehicles"

[10] FMVSS 304, NHTSA. "Compressed natural gas fuel container integrity"

Considerations Regarding Electric and Hybrid Vehicle Safety

Donald Parker
Celina Mikolajczak
Robert Lange
Exponent, Inc.
USA
Paper 11-0117

ABSTRACT

Lithium-ion batteries are often the preferred choice for powering rechargeable-battery-operated consumer products due to their high value proposition for cost and energy density. Lithium-ion batteries are also highly reliable. Therefore, lithium-ion battery packs are now finding their way into very complex consumer products including hybrid and electric vehicles. The utilization of lithium batteries in small consumer products is increasing rapidly. However, lithium-ion battery failures can be substantially more energetic than failures of conventional battery units traditionally used in the automotive market, due to higher quantities of stored electrical and chemical energy within lithium-ion cells.

The large and complex battery configurations needed for electric and hybrid vehicles and the applications to very demanding automotive operational conditions present new challenges in areas of safety, durability, reliability, and performance. Thus, the risk potential and exposure to new potential technical challenges in a new and demanding operational environment should be considered in the vehicle development process. As new uses are explored, this battery technology must be well understood and thoroughly considered in the context of the new application.

INTRODUCTION

The community of individuals and institutions with interests in motor vehicle safety is very large, including but not limited to:

- Vehicle drivers/ roadway users
- Motor vehicle manufacturers
- Safety researchers and practitioners
- Government institutions:
    - Legislative
    - Administrative
    - Judicial
    - Law enforcement
    - Transport officials
- Health officials
- Non-government organizations/institutions (NGOs)
- Emergency responders
- Roadway designers and builders
- Taxpayers

Historically, the role of vehicle safety could be defined by a Haddon matrix that plots the injury triangle elements of driver, environment and vehicle against timeframes before a crash, during a crash, and after a crash. The advent of electric vehicles (EVs) and hybrid electric vehicles (HEVs), both of which come in a variety of categories defined by their operating mechanism configurations, has added a new layer of health and safety concerns.

New elements to be considered include:

- Energy storage methods
- High voltage sources
- High power electrical connections and lines
- Battery chemistry
- Battery crashworthiness
    - Battery structure robustness
    - Battery protection within vehicle
- Service considerations
- Energy recharging
    - Vehicle manufacturer
    - End user
- Battery handling and shipping
- Battery storage at vehicle test and assembly facilities
- Information and knowledge transfer to affected parties

Due to energy density characteristics, lithium-ion cells are currently an attractive choice for assembling into high voltage rechargeable batteries for EV and HEV use. What is not so quick to penetrate, particularly in the view of the public and of non-technical but interested government entities as expressed in public media and blogs, is that the shift to lithium-ion batteries as a rechargeable power source is a major paradigm shift, and the learning curve for new applications can be both steep and challenging. An understanding of the cell chemistry, reliability safety performance and potential failure

modes and by-products form part of this learning curve.

DISCUSSION

While battery cells have been with us for hundreds and even thousands of years, most significant battery development for consumer products before the lithium-ion has been based on an aqueous electrolyte.

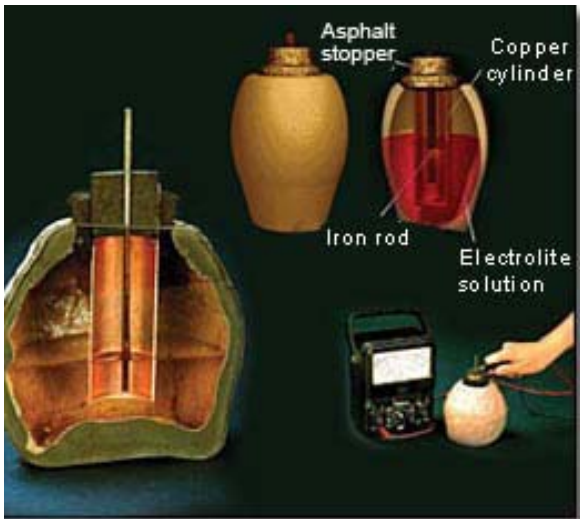

Figure 1. The "Baghdad Battery", from 200 BC Persia (speculated use)

Aqueous-based cells and batteries can produce flammable gases, usually hydrogen gas produced by electrolysis of water, during charging and operation, and can be consumed in a fire. Lithium-ion batteries, however, contain flammable organic electrolyte that can release significant chemical energy upon combustion.

Lithium-ion batteries have been commercially available since the early 1990s. Since that time lithium-ion chemistry has become the dominant battery chemistry in a wide variety of consumer electronic devices. Adopting lithium-ion technology to automotive applications can appear, in many respects, to be a straightforward problem of scaling up an existing technology. However, there are a number of factors related to actual experience with lithium-ion cells compared to automotive industry performance requirements, current lithium-ion battery technology itself, as well as various potential issues with scale-up that may prove problematic.

Automotive requirements are significantly more demanding than those imposed on today's consumer electronics lithium-ion battery packs. Consumer electronics devices range in size and complexity from very small single cell devices (e.g., Bluetooth headsets, hearing aids) to multi-cell devices with elements connected in series. Very small cell devices run at nominal voltages of 3.7 V, with capacities in the range of 0.05 Ah (0.19 Wh), with rudimentary protection electronics.

Multi-cell devices such as notebook computer battery packs run at nominal voltages of up to 14.4 V with capacities up to 6.6 Ah (95 Wh) and higher, and implement complex protection electronics. Notebook computers arguably represent the largest population of relatively complex lithium-ion batteries in the commercial market. Most of these packs contain between three and sixteen individual cells connected in combinations of series and parallel cell stacks. It is therefore not un common to find pack configurations involving three- or four-series cell blocks with each block consisting of two or more cells connected in parallel. There are some notebook computer battery packs and power tool battery packs, which include larger cells or higher cell counts.

The maximum size of commercially available portable product battery packs has been effectively limited by international shipping regulations (ref. 1). Exemptions to hazardous materials transport rules for lithium-ion cells smaller than 20 Wh (effectively a 5 Ah cell with a nominal voltage of 3.7 V) and lithium-ion batteries smaller than 100 Wh (e.g., a battery pack with twelve 18650 cells of 2.2 Ah capacity each) are listed. Cells or battery packs that fall outside of the exemption limits must be transported as Hazardous Materials. Due to the generally smaller size of consumer products and their batteries, it can be argued that small form factor batteries make up the bulk of the market. The consumer products industry now has more than 20 years experience with small form factor cells, such that cell quality (manufacturing) and protection electronics (battery pack design) interact to generally result in adequate cell performance.

In comparison, based on the total number of vehicle manufacturers utilizing large-format lithium-ion cells in service, it can be argued that there is very limited experience with high volume large format (ref 2) Lithium ion cells or large parallel arrays of cells. A

small number (relative to typical consumer product battery pack populations) of larger lithium-ion battery packs have been manufactured for certain low volume (at the time of this writing) applications such as electric vehicles, satellites, grid stabilization applications, and military applications. Some of these large battery packs have been constructed using cells common to commercial applications. These designs involve connecting more than one cell in parallel to form elements or blocks that are then connected in series. Other large battery packs have been constructed from "large format cells" that have capacities in the range of 10 Ah to 100 Ah.

There is a whole lithium-ion cell family to consider; consisting of numerous lithium-ion cell chemistries being developed and deployed in consumer products of all kinds, ranging from tiny single-cell button batteries used in small consumer products such as wireless headsets to large EV batteries consisting of thousands of cells and producing hundreds of volts. What all practical or currently commercially available lithium-ion batteries have in common in varying degrees is: 1) Organic electrolyte; 2) Strong oxidizers and reducers, and; 3) No ion recombination rate ability. Due to their chemistry, all commercially available lithium-ion batteries exhibit a sensitivity to heat which can trigger a self-supporting exothermic chemical reaction and thermal runaway. Therefore, during normal operation, fail-safe controls applied directly to the batteries are required to control and limit such reactions during foreseeable use and abuse conditions.

Cell chemistry affects the stability and volatility of the cells. In very general terms, more volatile cell chemistries provide a greater energy density by mass, but can present a higher risk of a thermal runaway event. More stabile cell chemistries provide a higher threshold to thermal runaway, but generally also have lower energy density, which requires a bigger battery for equivalent energy - thus potentially more chemical fuel if a fire does occur.

Severe battery failures (failures that can cause injury; e.g., thermal runaway, cell venting, venting with flames) are rare events: it has been Exponent experience that a 1-in-1-million failure rate (for severe failures) has historically been considered a minimally acceptable rate by the US Consumer Product Safety Commission (CPSC). Batteries have been recalled if a defect in the battery that has injury potential was identified. A typical severe consumer electronics device battery failure is generally limited to the device and its immediate surroundings. Most resulting fires, if they occur, can be controlled with a hand extinguisher or equivalent, unless, for instance, undetected and allowed to progress into a house or building fire. Severe failure of a large format battery will likely pose a significantly greater hazard simply due to the increased volume of potentially hazardous and flammable vent gas produced by reacting cells and increased electrical energy available.

Note that severe cell failures can be caused by a multitude of failure modes (ref. 3) associated with deficient cell design, cell manufacturing defects, mechanical or thermal damage, user abuse, or other issues. Relative to consumer electronics applications, the automotive environment poses increased risk of mechanical damage to batteries due to operation in a highly dynamic environment, and the potential for direct or indirect collision-related insult. Additionally, thermal stress subsequent to a collision and ignition of non-battery components of the vehicle could occur. Thus, even if they had comparable cell and battery pack designs and manufacturing defect rates, the automotive industry might experience an increased rate of severe cell failures, greater than that seen in consumer electronics. Therefore, vehicle manufacturers must forecast these potentials and act to reduce the likelihood of occurrence. To maintain comparable severe failure rates, automotive battery designs must be designed to be even more robust and tolerant to factors such as internal faults and external damage than current commercial battery designs.

In many cases, the cells are produced by one independent company, which provides them to a second independent company which packages them together into a battery or power unit, perhaps with built-in electronic thermal sensors and other controls, which are then provided to a final manufacturer for assembly into a vehicle or other product. This can make root cause analysis and application of production system corrections challenging, particularly in a rechargeable battery environment where a fault may not propagate itself until years after fabrication. Systems for accurately back-tracking manufactured cell lots used in battery pack assembly will be critical. Motor vehicle manufacturers are already accustomed to this supply chain sequence and have sophisticated tracking mechanisms to look down the supply chain to locate original sources.

A subset of this paradigm shift is also to understand how to respond to an emergency situation involving lithium-ion batteries, particularly as envisioned for use in automotive products. Something as straight forward as fire suppression becomes a difficult

question to which there is common consensus opinion. Historical experience with consumer product lithium-ion batteries, does not necessarily apply. There is little field experience with fire suppression of large-format lithium-ion batteries. In general, the best way to extinguish a lithium-ion battery fire is to extract the heat from the chemical reaction. Water has good cooling properties, yet to flood a high-voltage battery with water has potential hazards and limitations of its own, and it is not known how these concerns are addressed in current rescue/firefighting codes and protocols.

Analysis and testing is also required to understand the potential organic by-products of a runaway chemical reaction for a specific cell chemistry, what potentially harmful gases may be vented and in what quantities.

There are many areas of concern where there is very limited public field experience with lithium-ion batteries as a power source in volume automotive production, and issues tend to change as production moves from low-volume prototype testing, where batteries are typically manufactured and assembled with temporary tooling or by hand, to high-volume production with many automated operations. The risk tends to evolve, and the lack of a product failure modes knowledge base hinders facilitation of mitigating actions.

Failures of cells/batteries can have various effects of various severities, but that could include: loss of function of the product or vehicle; property damage to the device or vehicle itself; property damage to a manufacturing plant or test facility; property damage to the house or building where the product or vehicle is being used or stored and/or charged; and personal injury or death due to combustion and/or chemical reaction by-products such as harmful gases.

Lithium-Ion Battery Technology

Although scaling-up existing lithium-ion technology may seem to be relatively straightforward, as noted earlier, various potential issues may be problematic. As an illustration we present two examples of the difficulties involved in scaling up lithium-ion technology for application in EVs and HEVs; maintaining cell electrode coating quality, and adopting battery protection approaches from consumer electronic devices.

The term lithium-ion battery refers to a family of battery chemistries where the negative electrode and positive electrode materials serve as a host for the lithium-ion (Li^+). Like a lithium metal battery (lithium metal negative electrode), a lithium-ion cell provides a high-energy density and a high-voltage potential. These batteries differ from lithium metal batteries in that lithium-ion cells use lithium intercalation compounds as the negative electrode material rather than metallic lithium. Use of intercalation compounds for electrodes does reduce energy density relative to lithium metal systems, but it possible to recharge the battery over hundreds of cycles (ref. 4). The lithium intercalation sites in the negative and positive electrodes are at different chemical potentials; therefore, discharge is spontaneous and limited by diffusion. In this system, the useful energy comes from electrons moving to a lower electrical potential while compensating for the transfer of positively charged lithium from the high chemical potential intercalation material to the lower chemical potential intercalation material.

The four primary functional components of a practical lithium-ion cell are the negative electrode (anode), positive electrode (cathode), separator, and electrolyte. Additional components of lithium-ion cells such as the current collectors, case or pouch, internal insulators, headers, and vent ports can also impact cell reliability and safety. The chemistry and design of all of these components can vary widely across multiple parameters. The market is currently dominated by lithium-ion cells that have similar designs: a negative electrode made from carbon/graphite coated onto a copper current collector, a metal oxide positive electrode coated onto an aluminum current collector, a polymeric separator, and an electrolyte composed of a lithium salt in an organic solvent. For the purposes of this paper, the discussion will be limited to these types of lithium-ion cells.

The lithium-ion cell negative electrode is composed of carbon/graphite powders combined with a binder material that is coated in thin layers onto a metal foil current collector. The nature of the carbon can vary considerably: in particle size, particle size distribution, particle shapes, particle porosity, crystalline phase of carbon, etc. The negative electrode material mixing and coating process is often proprietary as variations in processing parameters will affect the resultant coating, and have a strong effect on cell capacity, rate capability, and ageing behavior.

There are varieties of positive electrode materials used in traditional lithium-ion cells – as with the negative electrode, these materials are powders that are combined with conductivity enhancers (carbon) and binder, and coated in a thin layer onto a foil current collector. The most common material is lithium cobalt dioxide (a layered oxide). However, various other materials are used such as lithium iron

phosphate, spinels, such as lithium manganese (Mn) oxide, or mixed metal oxides that include cobalt (Co), nickel (Ni), aluminum (Al), and manganese oxides.

The electrolyte in a traditional lithium-ion cell is typically a mixture of organic carbonates such as ethylene carbonate or diethyl carbonate. These solvents contain solvated lithium-ions, which are provided by lithium salts such as lithium hexafluorophosphate ($LiPF_6$).

In a cell thermal runaway, electrolyte vents from a cell. The resulting vent gases are flammable due to the organic solvents, and may also be toxic due to the dissolved lithium salts. Much of the discussion surrounding safety of lithium-ion cells is directly related to the flammability of the electrolyte. Discussions of electrode stability, self-heating rate, resistance to over-charge, resistance to cell internal shorts, resistance to external shorts, resistance to crush (e.g., from automotive collisions), resistance to thermal abuse, and reliability of pack protection electronics are primarily driven by concern over the likelihood of cells undergoing thermal runaway reactions that cause venting of a flammable electrolyte. Ignition can also occur if the vent gases come into contact with any number of possible competent ignition sources including hot surfaces (possibly heated cell cases), sparks, or open flames. For example, garage spaces often contain heaters with pilot lights. Furthermore, the automotive industry must plan for severe vehicle collisions where numerous ignition sources exist such as sparks from metal scraping on pavement, lamp filaments, arcing of electric systems, etc.

The use of copper as the current collector for the negative electrode has particular reliability and safety implications. At severe levels of battery discharge, usually ~ 1 V for the cell, the copper current collector will begin to oxidize and dissolve. On subsequent recharge, the dissolved copper plates onto negative electrode surfaces, reducing their permeability and making the cell susceptible to lithium plating and capacity loss. Usually, once a severe over-discharge event has occurred, cell degradation accelerates because once the negative electrode has become damaged by copper plating it will no longer be able to uptake lithium under "normal" charge rates. In such an instance, "normal" charge cycles cause lithium plating, which result in a greater loss of permeability of the surfaces. Ultimately, over discharge of cells can lead to cell thermal runaway.

Most consumer electronics devices set specific discharge limits for their lithium-ion battery packs to generally prevent over-discharge. The protection electronics disconnect the pack from the discharge load, but they cannot prevent over-discharge resulting from self discharge of cells. Thus, if a device is fully discharged and then stored for an extended period, the cells may become over-discharged, or if a mild short exists within the battery, the cells may become over-discharged within a short time. Most pack protection electronics will allow recharge of over-discharged cells, despite the potential for the negative electrode to have become damaged. In single cell consumer applications (e.g., cell phones), the resulting capacity fade, and elevated impedance of the battery will generally drive a user to replace the battery pack. Nonetheless, over-discharge does periodically cause thermal runaway of single cell battery packs. In multi-series element battery packs (e.g., notebook computers), the capacity fade, and elevated impedance will usually cause a severe block imbalance that drives permanent disabling of the battery pack.

Electrode Quality

Practical lithium-ion cell and battery pack lifetimes are strongly related to electrode coating uniformity. A uniform electrode coating will ensure that electrode material from all parts of a single cell performs in the same way: that one portion of the electrode is not being over-charged or over-discharged, while another portion of the electrode remains within an acceptable operational envelope, particularly as the cell ages. Localized overcharge or over-discharge within a cell could lead to reliability and safety problems.

Uniform electrode coatings also result in cells that have well matched capacities and internal impedances that will perform well when assembled into large battery packs. On commercial cell production lines, after cells are manufactured (and also sometimes before they are assembled into battery packs), cells are tested for capacity and impedance, and then graded based on these parameters. Severe outliers are rejected. This grading and matching process serves to group together cells with uniform qualities "as tested" in 2 to 3 Ah segments. As long as the cells are properly matched, batteries produced from them will perform well even with tight cut-off voltages.

If an electrode coating process produces variability; for example, coating thickness increases steadily from one end of a roll to another, small cells produced from the beginning of a roll will likely match each other and internally contain fairly uniform electrodes, while small cells produced from the end portion of the roll will likely match each other and internally contain fairly uniform electrodes,

but small cells produced from the beginning of the roll will likely not match small cells produced from the end of the roll (Figures 2 and 3). Large cells produced from the same roll would likely be more difficult to match, and in addition, their internal electrodes could exhibit more significant variability. The presence of this greater variability would require the application of more gracious cut-off voltages – effectively "derating" a battery pack and increasing cost per capacity.

When impedance is measured across a large format cell or a large parallel array of cells, the resulting values are the average of values across all of the electrodes and parallel cells. Similarly, the capacity of a large format cell or a large parallel array of cells is an average of the capacity of the entire electrode area. Thus, a zone of high impedance (or low capacity) on a small part of an electrode or within a single cell in a large parallel array, will appear identical to a modest impedance increase (or a modest capacity decrease) over the entire electrode or all cells within a parallel array.

In consumer electronics battery packs, independent voltage sensing (and thus, calculated capacity and cell impedance) occurs at each block element resulting in approximately one voltage sensor per 5 Ah of installed capacity. In comparison, for a ten 18650 cell block there will be one voltage sensor per 25 Ah of capacity, and for a large format cell there might be one sensor per 50 Ah of capacity: a reduction of sensor "density" by a factor of 10. Should a relatively high impedance (or low capacity) zone form within a larger cell or a large parallel array of cells, it will be undetectable via this measurement approach. However, the presence of even small high impedance or low capacity zones may result in electrode degradation that can accelerate cell aging, and possibly cell thermal runaway.

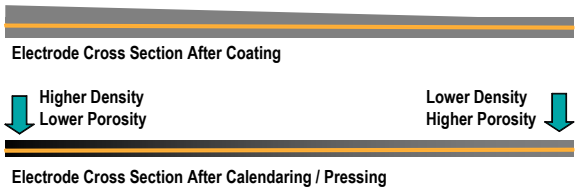

Figure 2. Effects of non-uniform coating on electrode density and porosity

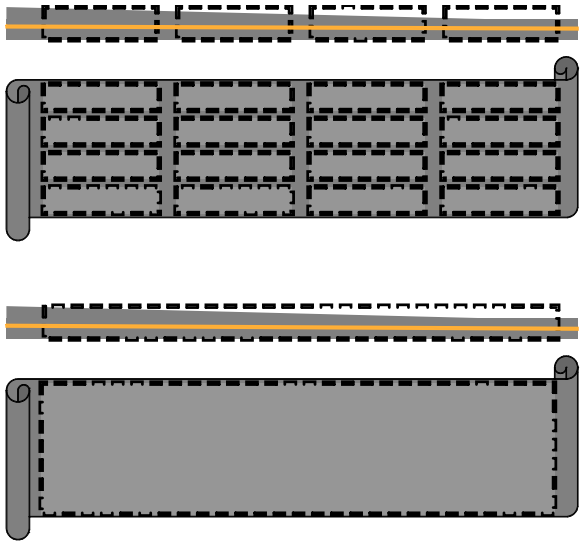

Figure 3. Schematic depiction of an electrode roll with large-scale coating thickness variation, and the effect of that variation on small and large format electrodes cut from the roll.

Beyond the challenges associated with large scale coating variation, defects in coatings that can cause cell failures (Figure) are more likely to be detected during grading of small cells as the size of defect that is detectable scales more favorably with the area of electrode that is being tested. Thus, production of large format cells with quality comparable to typical commercial cells requires tighter control of a range of coating processing parameters than for production of small commercial cells.

If an internal short occurs within a cell, the shorting location can draw energy from the entire cell, as well as any cells connected in parallel. Thus, a short that may result in a very mild failure in a small single cell, may result in a severe failure in a multi-cell configuration or in a large format cell. To date, Exponent is unaware of any testing conducted to assess the potential effect of cell capacities or high parallel cell counts on internal cell faults. There is also insufficient field data available to assess this issue.

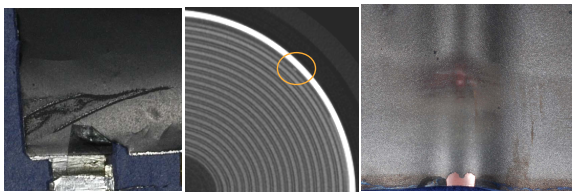

Figure 4. Three examples of coating defects: scratch, contaminant, delamination or void.

Battery Safety Devices

Consumer electronics battery packs rely on a number of safety devices to disable cells and battery packs that may have become degraded and could pose a risk of thermal runaway. Not all of these devices are compatible with large battery packs. For example, some small commercial cells, such as 18650s, integrate charge interrupt devices (CIDs).

On activation CIDs physically and irreversibly disconnect the cell from the circuit. Although CIDs are usually described as overcharge protection devices, they will activate if anything causes cell internal pressure to exceed the activation limit. This could include overcharge, cell overheating, significant lithium plating, mild internal shorting, and/or significant cell over-discharge. Should a CID activate in a large parallel array of cells, it will cause redistribution of the full current to other cells in the array. In two or three cell parallel arrays, CID's generally work as expected and facilitate a graceful failure of a battery pack. Ideally, if a significant fault condition were encountered, all CIDs in a parallel array would activate simultaneously.

In practice, however, these devices do not activate simultaneously, which can result in high current application to a small subset of array cells with non-activated safety devices, leading to over-current over-charge conditions that can cause cell thermal runaway (Ref. 8).

In most consumer electronics applications, a benign battery failure (e.g., loss of capacity, or inability to recharge) is viewed as a nuisance rather than a critical failure. Thus pack protection electronics in notebook computers generally are capable of permanently disabling a battery pack if certain conditions are detected including a variety of out-of-range conditions such as excessive pack temperature, as well as when the functionality of various components is in doubt, in order to produce graceful failure of a battery pack rather than a severe failure.

The permanent disable features in notebook computers also effectively provide a mechanism for acceptable premature end-of-life of these battery packs. For example, one of the conditions that will cause permanent disabling of a notebook computer battery pack is a severe block imbalance: the pack is disabled if there is a significant voltage divergence between series elements (blocks) within the pack. Block imbalance detection is often discussed in literature as a redundant method for preventing cell over-charge. However, in practice, block imbalance detection serves to detect cells that have become damaged, for example, by severe over-discharge, internal shorting, electrolyte leakage, etc. Continued cycling of cell blocks containing damaged cells could result in thermal runaway reactions. In automotive applications, with many blocks in series and many series strings in parallel, permanent battery pack disabling may be required if block voltages become too unbalanced.

CONCLUSIONS

Despite a long and largely successful history in consumer electronics devices, the use of lithium-ion cells in automotive applications continues to pose a range of challenges, a few of which have been discussed here. There is very limited public field experience with lithium-ion batteries as a power source in automotive products. Protocols for shipping and handling large format batteries in various states of charge are in their infancy, as well as those for emergency response to large format battery fires. One of the main challenges in solving the technical issues will be to identify and fully address risk elements that attach to use of lithium-ion technology batteries in the automotive environment. Prior experience with smaller scale consumer product applications can serve as guidance to these risk considerations and other analytical techniques may assist in identifying and evaluating risks to be addressed.

REFERENCES

1. UN Transport of Dangerous Goods – Model Regulations, ICAO Technical Instruction for the Safe Transport of Dangerous Goods by Air, IATA Dangerous Goods Regulations, etc.
2. The term "large format" is often loosely applied in the lithium-ion battery area, as the definition is linked to transport regulatory requirements that have been subject to change. Based on recent UN Model Regulations, a large format cell contains more than 20 hr of energy (for example, more than 5 Ah capacity with a 3.7 nominal voltage), while a large format battery pack contains more than 100 Wh of energy (for example, a battery pack containing more than twelve 2.2 hr cells).
3. Mikolajczak C, Stewart S, Harmon, J, Horn, Q, White K, Wu M, Mechanisms of latent internal cell fault formation and opportunities for detection, Proceedings, 2008 NASA Aerospace Battery Workshop, Huntsville, AL, November 18–20, 2008 and Mikolajczak C, Stewart S, Harmon, J, Horn, Q, White K, Wu M, Mechanisms of latent internal cell fault formation, Proceedings, 9th BATTERIES Exhibition and Conference, Nice, France, October 8–10, 2008.

4. Attempts to manufacture practical rechargeable lithium metal batteries with cycle life greater than 300 cycles have generally proven unsuccessful to date due to uneven lithium plating (dendrite formation) during charging.
5. Kishiyama C, et al, "Improvement of Deep Discharge Capability for Lithium Ion Batteries," Abs. 425, 204th Meeting, The Electrochemical Society, Inc., 2003.
6. Zhao M, et al., "Electrochemical Stability of Copper in Lithium-Ion Battery Electrolytes," *Journal of the Electrochemical Society*, **147** (8) (2000) 2874-2879.
7. A PTC device may serve to limit the current available to a shorting cell.
8. Jeevarajan J, "Performance and Safety Tests on Lithium-Ion Cells Arranged in a Matrix Design Configuration," Space Power Workshop, April 2010.

WHY SHOULD ALUMINUM CONTINUE TO REPLACE STEEL IN CARS? AN LCA (LYFE CYCLE ASSESSMENT) COMPARISON

Gustavo Zini
School of Engineering – University of Buenos Aires
Argentina
Paper Number 11-0167

ABSTRACT

"To achieve more sustainable production and consumption patterns, we must consider the environmental implications of the whole supply-chain of products, both goods and services, their use, and waste management, i.e. their entire life cycle from 'cradle to grave' ". (Preface to the ILCD Handbook: General guide for Life Cycle Assessment)

Though conventional wisdom states that more fuel-efficient vehicles are lighter and smaller, yet less safe than their less fuel-efficient counterparts, another point of view will be shown. Aluminum and other materials have proven to replace steel with a good trade-off of fuel efficiency against safety. Yet steel is predominant in mass production automobiles, representing around 65% of their weight. The reasons behind this choice could be explained through both cost effectiveness and technology expertise, but they will not be thoroughly analyzed in this paper. However, it can be argued that a complete assessment of the ecological impact of using aluminum instead steel has not been done up till now, or at least has not been taken into full consideration. The use of lighter yet impact-efficient materials will certainly improve both safety and fuel economy, so a comprehensive study in this issue is proposed.

Therefore, this paper will compare the LCA (Life Cycle Assessment) of two different cars, one with a steel chassis group and body-in white, and another one having these parts made out of aluminum. This comparison has already been made by the University of California [1]. Nevertheless, a different approach is hereby proposed, so that both conclusions can be contrasted.

To conclude, a new LCA model will be developed, and two hypothetical vehicles will be compared on a theoretical approach, pointing out some aspects that should be developed thoroughly within the corresponding settings and using appropriate resources.

INTRODUCTION

"Design is the process of devising a system, component, or process to meet desired needs. It is a decision making process (often iterative), in which the basic sciences, mathematics, and engineering sciences are applied to convert resources optimally to meet a stated objective. Among the fundamental elements of the design process are: the establishment of objectives and criteria, synthesis, analysis, construction, testing and evaluation." (ABET: Accreditation Board for Engineering and Technology, 1988)

Weight does matter.

On the one hand, lighter automobiles mean lower fuel consumption and therefore minor impact to the Environment. Yet this is only partly true, because in order to fully understand the mentioned impact an assessment of the complete product life-cycle must be done. For example, an electric motor generates no CO_2 emissions, yet the electricity that is stored in the batteries could have been generated in power plants that use either more energy or green-house gasses than an internal combustion energy. A life cycle assessment is a technique to assess each and every impact associated with all the stages of a process from cradle-to-grave. LCA's can help avoid a narrow outlook on environmental, social and economic concerns.

On the other hand, fuel-efficient engines also generate lower impact to the Environment. As time passes, automobile engines are getting smaller, lighter, and more fuel-efficient than ever.

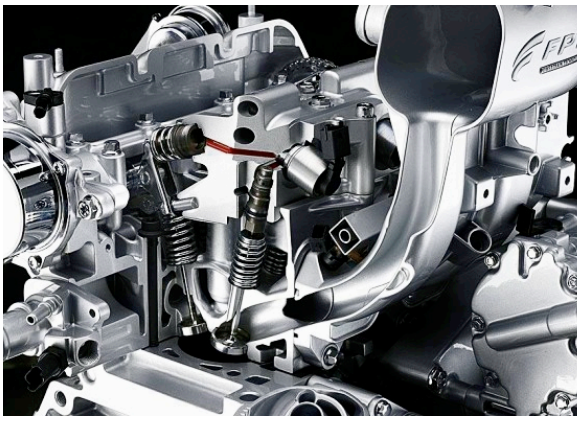

Figure 1. FIAT's new Twin-Air engine.

For example, using next-generation technology, the new Fiat "Twin-air" engine implements a revolutionary system, taking the concept of downsizing to the extreme and masterly tuning the basic mechanics, the new family –delivering from 65 to 105 HP– emits 30% less CO_2 than an engine of equal performance.

Therefore, it can be stated that modern engines are both less fuel-consuming devices and more environmentally-friendly. Yet, and this can be highlighted as one of the key issues discussed in this paper, automobiles are getting heavier and heavier. For example, and as expressed by the European Aluminium Association, the average mass of European vehicles has dramatically increased. The weight increase is basically due to more stringent legislative requirements and changing customer demands (growing vehicle size, extra comfort and safety devices, etc) that, in turn, have caused an increase weight of other components to reach the envisaged performance level. This "weight spiral" is shown in the next figure [2].

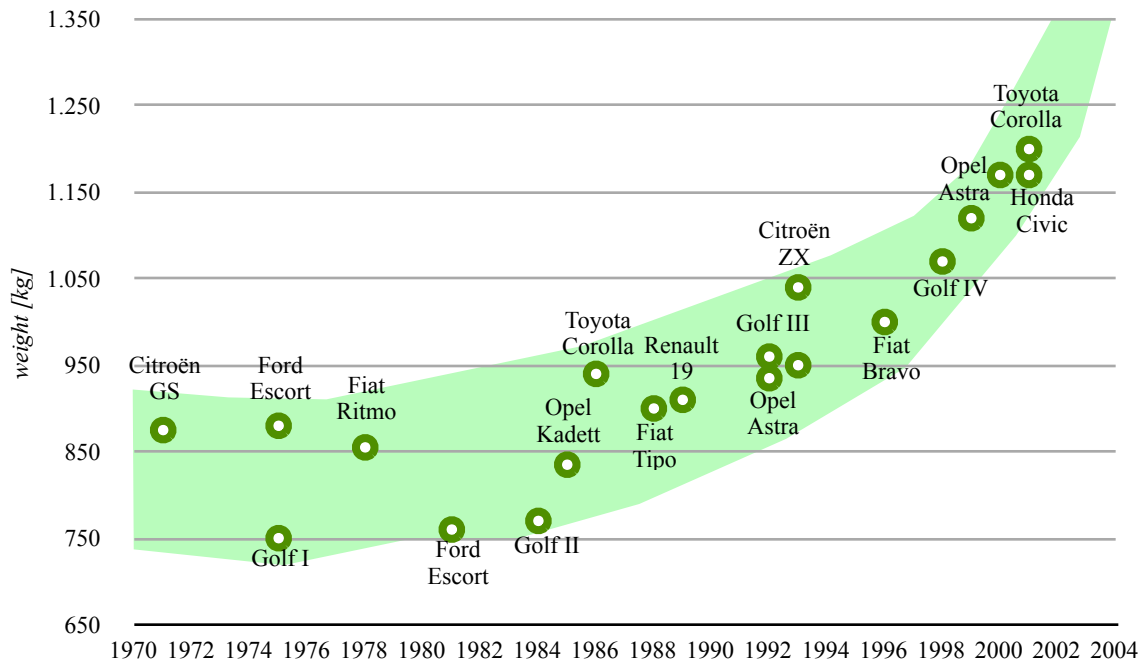

Figure 2. Passenger car mass distribution from 1970.

Consequently, if there is a clear advantage in weight reduction. why are innovation efforts concentrated on designing better engines but not lighter automobiles? Why is it that no high-volume mass-production vehicle is made entirely in aluminum? These answers exceed the purpose of this paper, but it has to be pointed out that even though it is crystal clear that wider use of aluminum will mean lighter vehicles and lower fuel consumption, is it worthy to outclass every technological and economical motive that excluded aluminum from high-volume production? Will the Environmental impact of this action compensate the disadvantages that have until nowadays maintained steel as the principal material used for automobile manufacturing? These two latest questions are the ones that will be answered, or at least an outline of the answers will be given.

In order to do so, two papers [1]; [3] will be used as a basis to perform this particular study.

Figure 3. AUDI's A2 had an all-aluminum body frame.

The first one of them will give an indication of the percentage that each part of an automobile bears in terms of weight distribution:

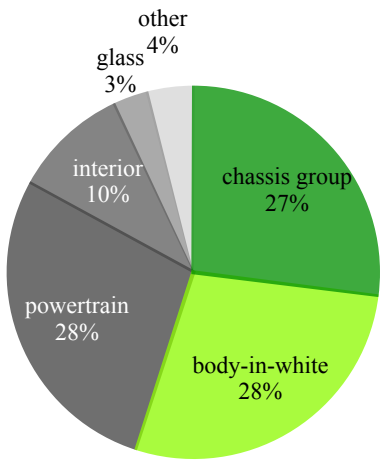

Figure 4. Passenger car mass distribution [3].

It also states that aluminum has reached its limit in substituting steel both in the powertrain and in the interior parts, but has a very minor use in the chassis group and in the body-in.white, which represent 55% of an automobile mass.

The other paper, developed by the World Steel Association analysis the LCA of three types of automobiles, two made out mainly of steel and one of aluminum [1].

A key finding of the latter paper is that with reasonable assumptions and inputs for the specific application and manufacturing processes, the material production phase can be a significant percentage of the vehicle's total carbon footprint. In fact, it becomes even more important as the vehicle's footprint is diminished through advanced powertrains and fuel sources. It also says that significant improvements in reducing automotive GHG emissions will not be achieved by material substitution alone; investment in new powertrains and fuels contribute to the greatest emissions reductions.

In other words, this study indicates that the use-phase of LCA has a lower impact than the other phases, which will be proven in this paper that could be an inaccurate statement.

Consequently, the calculation logic of the World Steel Association paper will be studied and remade, not to expose its probable inaccuracy, but to show that the energy consumed and the green-house gasses emissions during the product-use phase are several times higher than the ones of the other three phases of the LCA, and that this reason alone may justify a wider use of aluminum in the chassis group and in the body-in-white.

MODEL CARS AND TYPE OF ANALYSIS

"External goods have a limit, like any other instrument, and all things useful are of such a nature that where there is too much of them they must either do harm, or at any rate be of no use". (Aristotle, Politics, Bk 7 Chapter 1)

As said before, most of the findings of this paper are based on a reinterpretation of the data of papers [1] and [3]. An interesting issue to be mentioned is that the eventual substitution of steel by aluminum is analyzed by using a study from a Steel Association, thus minimizing the eventual bias that could be introduced if the data where taken from an Aluminum Association.

"The Impact of Material Choice in Vehicle Design on Life Cycle Greenhouse Gas emissions - The Case of HSS and AHSS versus Aluminum for BIW applications." compares three different cars, and there LCA. Herein, only two of the vehicles will be used, for simplification matters. The characteristics of the two automobiles that will be analyzed can be summarized in the following chart:

Table 1.
Characteristics of two of the automobiles used in reference [1].

	chassis group and body-in-white	
	steel	aluminum
steel [kg]	819,0	437,4
aluminum [kg]	88,2	282,6
other [kg]	352,8	352,8
total mass [kg]	**1.260,0**	**1.072,8**

It is interesting to point out that although the specific mass of aluminum is 1/3 of the one of steel (around 2.700 kg/m3 for Al versus 7.800 kg/m3 for Fe), lower tension- resistance results in that an automobile with a chassis group and body-in-white made out of aluminum will no be 65% lighter, but 30% instead. This statements is shared both by references [1] and [3]. And this reduction is not meant to be considered for the whole vehicle, but only for the chassis group and the body-in-white.

Hence, on the one hand, only two automobiles will be compared, one with its chassis group and body-in-white made out completely of steel, the other one made out completely of aluminum. To further simplify the analysis, all other materials will be taken out of the equations, as to perform a marginal analysis. It can be stated that this method of comparison will show the relative impact of the use of each material with a higher precision and with a simpler and more accurate vision.

The following table, which is derived from table 1, shows the new material distribution of the two vehicles that will be analyzed in this paper:

Table 2.
Characteristics of two of the automobiles used in this paper.

	chassis group and body-in-white			
	steel		aluminum	
steel [kg]	819,0	90%	437,4	61%
aluminum [kg]	88,2	10%	282,6	39%
total mass [kg]	**907,2**		**720,0**	
			-20,6%	

It is very important to highlight that even though the "aluminum" car has a chassis group and a body-in-white made out of this material, 61% of its weight is all the same represented by steel, since there are some parts of the vehicle where steel cannot be substituted. Similarly, the "steel" car has 10% of its weight in aluminum components. Bottom line, the two vehicles which LCA will be analyzed can be sketched as follows:

Figure 5. Car 1 - "Steel" vehicle to be analyzed.

Figure 6. Car 2 - "Aluminum" vehicle to be analyzed.

To conclude, and as shown in table 2, the difference in weight between the two hypothetical vehicles is around 20%, again a number far lower than the 65% difference between Al and Fe specific mass.

LCA: ADOPTED PROCEEDINGS

According to Wikipedia, the goal of LCA is to compare the full range of environmental and social damages assignable to products and services, to be able to choose the least burdensome one. At present it is a way to account for the effects of the cascade of technologies responsible for goods and services. It is limited to that, though, because the similar cascade of impacts from the commerce responsible for goods and services is unaccountable because what people do with money is unrecorded. As a consequence LCA succeeds in accurately measuring the impacts of the technology used for delivering products, but not the whole impact of making the economic choice of using it.

The term 'life cycle' refers to the notion that a fair, holistic assessment requires the assessment of raw material production, manufacture, distribution, use and disposal including all intervening transportation steps necessary or caused by the product's existence. The sum of all those steps –or phases– is the life cycle of the product. The concept also can be used to optimize the environmental performance of a single product (ecodesign) or to optimize the environmental performance of a company.

Common categories of assessed damages are global warming (greenhouse gases), acidification (soil and ocean), smog, ozone layer depletion, eutrophication, eco-toxicological and human-toxicological pollutants, habitat destruction, desertification, land use as well as depletion of minerals and fossil fuels.

LCA includes four stages:

1. Goal and Scope
2. Life Cycle Inventory
3. Life Cycle Impact Assessment
4. Interpretation

The stage that will be considered in this paper is the third one (Life Cycle Inventory), and the chosen variant is the one named "Cradle-to-grave". Furthermore, impact assessment has been divided into four phases:

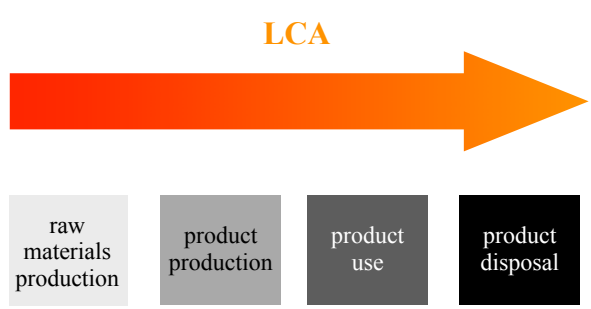

Figure 7. LCA impact assessment as considered in this paper.

FIRST PHASE: RAW MATERIALS PRODUCTION

The first assessment of the LCA is the energy and the amount of CO_2 that are consumed and released during the raw materials productions. The following table summarizes both parameters:

Table 3.
Energy consumption and green-house gas emissions for the production of primary and secondary steel and aluminum [1].

	total energy consumption [MJ/kg]	green-house gas emissions [kgCO_2eq/kg]
primary steel (basic oxygen)	21,7	2,0
secondary steel (electric arc furnace)	7,1	0,4
primary aluminum (electrolysis)	193,7	12,7
secondary aluminum (foundry)	10,3	0,6

Yet, every single part made out of aluminum or steel uses a certain percentage of primary and secondary metal. It can be stated, using as a general an very approximative rule that 40% of the steel used in the world is secondary, and that 30% of aluminum is secondary. Thereby, further considerations have to be made, starting by separating the above figures for primary and secondary metals:

Tables 4/5.
Use and energy consumption and green-house gas emissions for the production of primary and secondary steel and aluminum [1].

	primary		
	use	total energy consumption	green-house gas emissions
	%	[MJ/kg]	[kgCO_2eq/kg]
steel	60	21,7	2,0
aluminum	70	193,7	12,7

	secondary		
	use	total energy consumption	green-house gas emissions
	%	[MJ/kg]	[kgCO_2eq/kg]
steel	40	7,1	0,4
aluminum	30	10,3	0,6

After this, both total energy consumption and green-house emissions for the steel and aluminum used to build automobiles are integrated:

Table 6.
Energy consumption and green-house gas emissions for the production of steel and aluminum used in automobiles (considering the percentage of primary and secondary materials).

	primary and secondary	
	total energy consumption	green-house gas emissions
	[MJ/kg]	[kgCO_2eq/kg]
steel	15,9	1,4
aluminum	138,7	9,1

Thus, the figures for each hypothetical car result in:

Tables 7/8.
Energy consumption and green-house gas emissions for each of the hypothetical cars analyzed in this study (phase 1 of LCA).

	car 1		
	mass	total energy consumption	green-house gas emissions
	[kg]	[MJ]	[kgCO_2eq]
steel	819,0	13.022	1.147
aluminum	88,2	12.233	803
total	**907,2**	**25.255**	**1.949**

	car 2		
	mass	total energy consumption	green-house gas emissions
	[kg]	[MJ]	[kgCO_2eq]
steel	437,4	6.955	612
aluminum	282,6	39.197	2.572
total	**720,0**	**46.151**	**3.184**

The first issue to be highlighted is that the "steel" car has a lower environmental impact as far as phase 1 of the LCA is considered. This difference origins in the two completely different technologies used to obtain each metal from their mineral ore (basic-oxygen vs. electrolysis). The numbers from tables 7 and 8 can be transferred into a bar-chart that will be used throughout the entire paper:

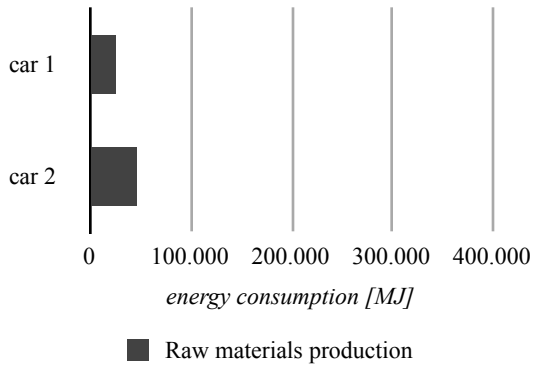

Figure 8. Energy consumption for LCA phase 1.

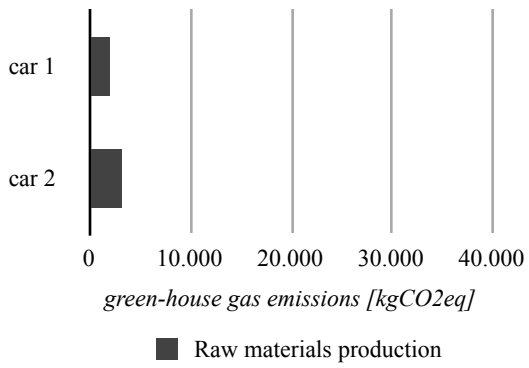

Figure 9. Green-house gas emissions for LCA phase 1.

SECOND PHASE: PRODUCT PRODUCTION

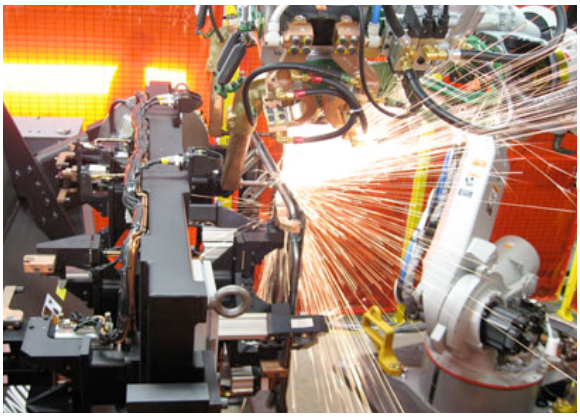

Figure 10. Production phase of an automobile.

Once the production of raw materials has been assessed, the transformation of these metals into the parts of an automobile will be analyzed. To do so, the proceedings of reference [1] will be adopted, as well as its data.

As in the previous and future phases of this LCA analysis, both the energy required to produce the mentioned parts and their carbon footprint during the production phase will be considered. The next two tables show the energy consumption and the green-house gas emissions for every type of steel and aluminum used in automobiles (namely flat carbon steel, cast iron, rolled aluminum, extruded aluminum):

Table 9.
Energy consumption during manufacturing for each type of material used in both hypothetical cars [MJ/kg].

	raw material	manufac-turing	**material in car**
flat carbon steel	15,4	9,8	**25,2**
long & special steel		5,4	**20,8**
cast iron		2,0	**17,4**
rolled aluminum	138,7	17,8	**156,5**
extruded aluminum		19,8	**158,5**
cast aluminum		12,2	**150,9**

Table 10.
Green-house gas emissions for each type of material used in both hypothetical cars [kgCO2eq/kg].

	raw material	manufac-turing	**material in car**
flat carbon steel	1,4	0,6	**2,0**
long & special steel		0,3	**1,7**
cast iron		0,2	**1,6**
rolled aluminum	9,1	1,2	**10,3**
extruded aluminum		1,2	**10,3**
cast aluminum		0,7	**9,8**

The above figures can be combined with the amount of each type of material used in the hypothetical cars that are been assessed (taking into consideration the proceedings of reference [1]) and merged into

the following tables that show the results of the second phase of the LCA:

Table 11.
Energy consumption and green-house gas emissions during manufacturing for car 1.

	mass [kg]	total energy consumption [MJ]	green-house gas emissions [kgCO_2eq]
flat carbon steel	504,0	4.939	302
long & special steel	189,0	1.021	57
cast iron	126,0	252	25
rolled aluminum	12,6	224	15
extruded aluminum	12,6	249	15
cast aluminum	63,0	769	44
total car 1	**907,2**	**7.454**	**459**

Table 12.
Energy consumption and green-house gas emissions during manufacturing for car 2.

	mass [kg]	total energy consumption [MJ]	green-house gas emissions [kgCO_2eq]
flat carbon steel	167,0	1.637	100
long & special steel	144,4	780	43
cast iron	126,0	252	25
rolled aluminum	159,5	2.839	191
extruded aluminum	73,1	1.447	88
cast aluminum	50,0	610	35
total car 1	**720,0**	**7.565**	**483**

In the same way that it was done after the first phase evaluation, the figures in the above tables will be transferred into a bar-chart that will show in a graphical way the differences between the environmental impact of each hypothetical car, for phases 1 and 2. Once more, and due to higher energy demanded on behalf of aluminum parts to be welded, a "steel" car proves to be more "environmentally friendly" than its "aluminum" counterpart, as it can be seen in the following graphs:

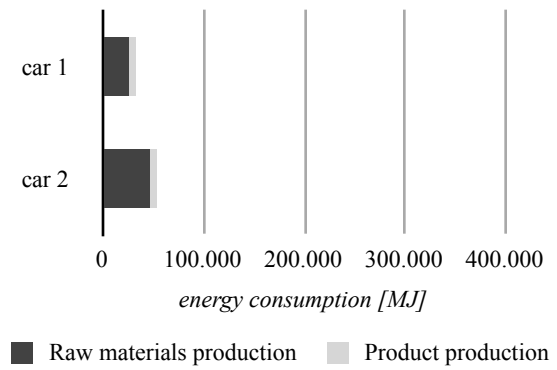

Figure 11. Energy consumption for LCA phases 1 and 2.

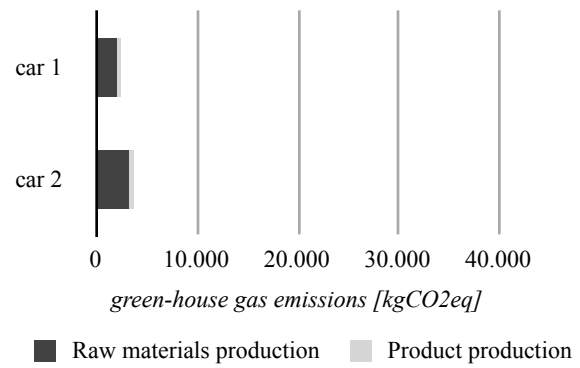

Figure 12. Green-house gas emissions for LCA phases 1 and 2 .

THIRD PHASE: PRODUCT USE

This phase of the assessment that marks the difference between the proceedings in reference [1] and this paper. As it will be shown in the conclusions, reference [1] takes into consideration that despite the fact that the "aluminum" car is lighter than the "steel" car, both fuel consumptions over the product use result in the same figures.

The parameters that can be found in different LCA assessments for the product use phase of an automobile consider traveling 200.000 km over a 10-year period. These figures are the same one used in reference [1] for the assessment, and in that case, the energy required to and the carbon footprint during the use phase for the "steel" car characterized in table 1 are the following:

➡ total mass [kg]: 1.260

➡ use [km]: 200.000

➡ energy consumption [MJ]: 407.700

➡ green-house gas emissions [kgCO_2eq]: 36.600

Nevertheless, it can be argued that it is very important to reconsider the difference in fuel consumption for different masses (as it may be obvious that lighter cars consume less fuel that heavier ones). Therefore, is it possible to conclude the percentage of fuel-consumption reduction that results from a mass reduction of an automobile?

To answer this question, the next chart shows that there is a statistically relevant correlation between car mass and fuel consumption:

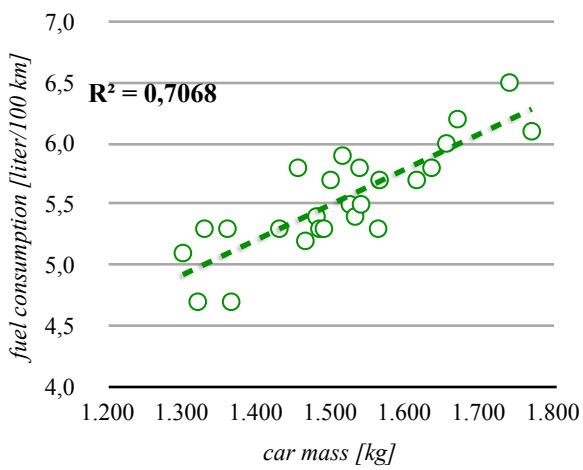

Figure 13. Correlation between car mass and fuel consumption for a sample of selected 2.0 (170 CV) diesel engine automobiles.

Every point of the chart is based on information provided by car manufacturers, for an average fuel consumption, has been taken from Quattroruote Magazine [4] and can be seen in Appendix I. Pearson's coefficient of 0,71 shows that there is a statistical relevant correlation between both parameters. From the regression equation it can be stated that for every 1% of mass reduction there is a 0,75% fuel consumption reduction:

➡ **1% mass reduction ⇒ 0,75% fuel consumption reduction.**

Using this parameter as an input to estimate the energy consumption and the green house gas emissions, which are directly related to fuel consumption, table 13 shows the figures for the original car in reference [1], and for the two hypothetical cars proposed in this paper, considering the above relationship between mass and fuel consumption. This figures can be considered as the key difference between the two studies herein compared.

Table 13.
Energy consumption and green-house gas emissions during product-use phase for cars 1 and 2.

	mass [kg]	total energy consumption [MJ]	green-house gas emissions [kgCO_2eq]
"steel" car from ref. [1]	1.260,0	407.700	36.600
car 1	907,2	**322.083**	**28.914**
car 2	720,0	**272.237**	**24.439**

As established, these numbers will be again transferred to a bar-chart:

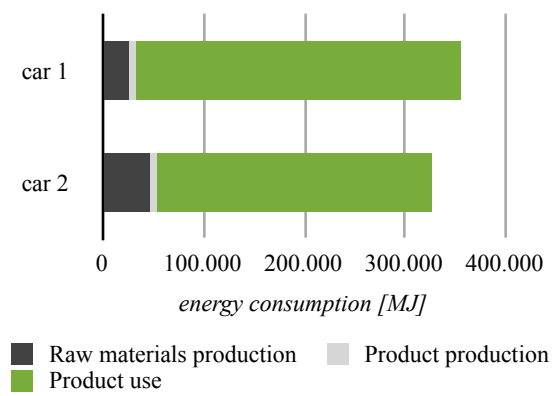

Figure 14. Energy consumption for LCA phases 1 to 3.

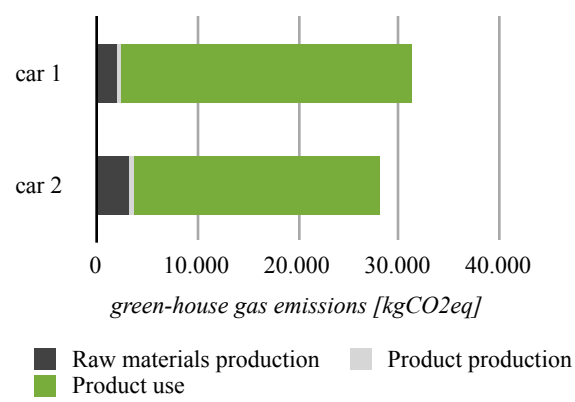

Figure 15. Green-house gas emissions for LCA phases 1 to 3.

For the first time in the analysis of this paper, the "aluminum" car proves to be more "ecologically-friendly". Furthermore, figures 14 and 15 show to what extent the product-use phase is by far the one that consumes more energy and emits more green-house gasses.

FORTH PHASE: PRODUCT DISPOSAL

In order to complete the LCA analysis in the variant called "Cradle-to-grave", product disposal must be assessed.

Using the figures from table 3, that indicate both energy consumption and green-house gasses emissions for secondary steel and aluminum, it is assumed that the entire mass of each hypothetical cars is scrapped as secondary metal. Hence, the impact of the fourth phase can be calculated as follow:

Tables 14/15.
Energy consumption and green-house gas emissions during product-disposal phase for cars 1 and 2.

	car 1		
	mass	total energy consumption	green-house gas emissions
	[kg]	[MJ]	[kgCO_2eq]
steel	819,0	5.815	328
aluminum	88,2	908	53
total	**907,2**	**6.723**	**381**

	car 2		
	mass	total energy consumption	green-house gas emissions
	[kg]	[MJ]	[kgCO_2eq]
steel	437,4	3.106	175
aluminum	282,6	2.911	170
total	**720,0**	**6.016**	**345**

As it could be already be deducted from table 3, there is practically no difference for each material, since both the energy required and the carbon footprint for recycling steel in an electric arc furnace and aluminum in a foundry are very similar.

To conclude, the numbers form tables 14 and 15 are added to the previous figures and shown in the following bar-charts. The final result of the LCA for both cars show that the "aluminum" one consumes 8,2% less energy during its life, while emitting 10,3% less green-house gases.

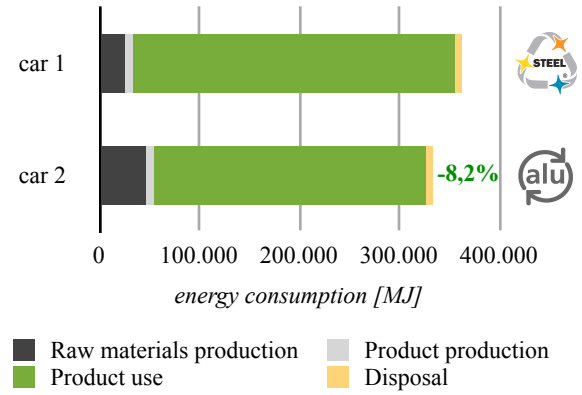

Figure 16. Energy consumption for entire LCA impact assessment stage.

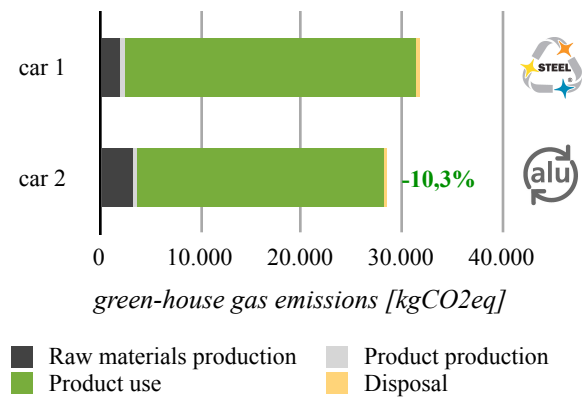

Figure 17. Green-house gas emissions for entire LCA impact assessment stage.

CONCLUSIONS

The aim of this paper was to compare the LCA of two different cars, one with a steel chassis group and body-in white, and another one having these parts made out of aluminum. As pointed out, this comparison has already been made by the University of California [1]. Nevertheless, the assessment in this paper had a different approach, so that both conclusions could be contrasted.

The first and most important contrast between the two studies is that while in reference [1] both the energy required and the carbon footprint where relatively

similar for each automobile, this paper indicates that the lighter vehicle in more environmentally-friendly:

Tables 16/17.
Total energy consumption and green-house gas emissions during the entire Life Cycle of the two hypothetical cars herein proposed.

	car 1	
	total energy consumption	green-house gas emissions
	[MJ/kg]	[kgCO2eq/kg]
raw materials	25.255	1.949
production	7.454	459
use	322.083	28.914
disposal	6.723	381
Total LCA	**361.515**	**31.703**

	car 2	
	total energy consumption	green-house gas emissions
	[MJ/kg]	[kgCO2eq/kg]
raw materials	46.151	3.184
production	7.565	483
use	272.237	24.439
disposal	6.016	345
Total LCA	**331.969**	**28.451**

Moreover, as said before, one of the key findings of reference [1] is that with reasonable assumptions and inputs for the specific application and manufacturing processes, the material production phase can be a significant percentage of the vehicle's total carbon footprint. In fact, it becomes even more important as the vehicle's footprint is diminished through advanced powertrains and fuel sources. This chart also clearly shows that significant improvements in reducing automotive GHG emissions will not be achieved by material substitution alone. Investment in new powertrains and fuels contribute to the greatest emissions reductions.

Yet, on the contrary, this paper clearly shows that the product-use phase impact outweighs by far the rest of the LCA phases, bearing between 80% and 90% of the total LCA impact:

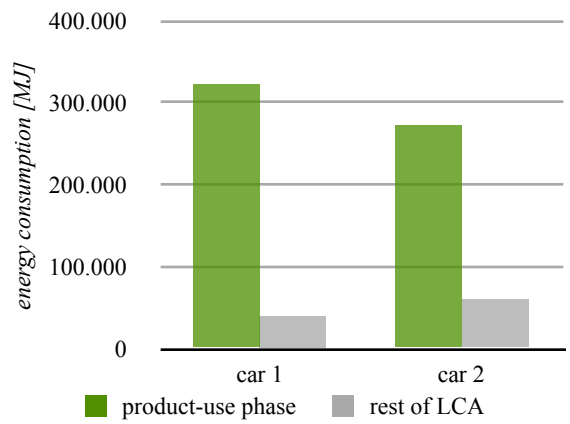

Figure 18. Energy consumption of product-use phase compared with the rest of the LCA phases.

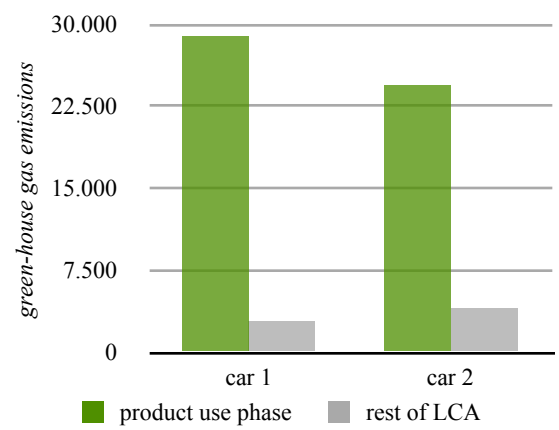

Figure 19. Green-house gas emissions of product-use phase compared with the rest of the LCA phases.

In other words, a car made out of aluminum instead of steel will generate a higher impact during its raw material and production phases, but a much lower impact during its product-use phase, and most important of all, a lower impact in its whole LCA.

On this basis it can be stated that as far as LCA assessment indicates, aluminum should continue to replace steel, specially in the parts of automobiles that is seldom used (chassis group and body-in-white).

To conclude, it is important to mention that the aspects herein pointed out where mostly analyzed in a theoretical and general point of view, and that they should be developed thoroughly within the corresponding settings and using appropriate resources for a proper comparison and conclusion.

ACKNOWLEDGMENTS

Professore Francesco Santarelli, Facoltà d'Ingegneria, Università di Bologna.

REFERENCES

(1) *Geyer, Roland. 2009. "The Impact of Material Choice in Vehicle Design on Life Cycle Greenhouse Gas emissions - The Case of HSS and AHSS versus Aluminum for BIW applications."*

(2) *European Aluminium Association. 2008. "Aluminum in cars."*

(3) *The Minerals, Metals & Materials Society - Journal of Materials. 2001. "Automobile Bodies: Can Aluminum Be an Economical Alternative to Steel?"*

(4) *Quattroruote Magazine, Italian Edition, march 2011.*

APPENDIX I - Fuel consumption for a sample of engines (2.0 diesel ≈ 170 CV) from reference [4].

brand	model	engine	power [CV]	mass [kg]	mean consumption [liter/100 km]
Alfa Romeo	Giuletta	2.0 JTD	170	1.320	4,7
	159 sedan/Brera			1.480	5,4
	159 SW			1.540	5,5
Audi	A3/A4 sedan	2.0 TDi	170	1.465	5,2
	A4 SW			1.525	5,5
	A6 sedan			1.565	5,7
	A6 SW			1.635	5,8
	A4 Allroad			1.670	6,2
Bmw	Serie 1	20d	177	1.365	4,7
	X1			1.490	5,3
	X3			1.740	6,5
Citroën	C5 sedan	2.0 HDi	163	1.563	5,3
	C8 sedan			1.770	6,1
Fiat	Bravo	2.0 Multijet	165	1.360	5,3
Ford	Mondeo sedan	2.0 TDCi	163	1.484	5,3
	S-Max			1.615	5,7
Lancia	Delta	2.0 MJT	165	1.430	5,3
Opel	Insignia sedan	2.0 CDTi	160	1.538	5,8
	Insignia SW			1.655	6,0
Peugeot	407 coupé	2.0 HDi	163	1.532	5,4
Seat	Exeo sedan	2.0 TDi	170	1.455	5,8
	Exeo SW			1.515	5,9
Volkswagen	Golf sedan	2.0 TDi	170	1.329	5,3
	Passat sedan			1.499	5,7
Volvo	S40	D4 2.0	177	1.300	5,1